

CONF 951071--1

1

**TRIBOLOGICAL PROPERTIES OF HARD CARBON  
FILMS ON ZIRCONIA CERAMICS\***

Ali Erdemir (Member, STLE), Cuma Bindal+, and George R. Fenske  
Tribology Section  
Energy Technology Division  
Argonne National Laboratory, Argonne, IL 60439

**RECEIVED**  
**JAN 30 1995**  
**OSTI**

Paul Wilbur  
Department of Mechanical Engineering  
Colorado State University  
Fort Collins, CO 80523

March 1995

**DISCLAIMER**

This report was prepared as an account of work sponsored by an agency of the United States Government. Neither the United States Government nor any agency thereof, nor any of their employees, makes any warranty, express or implied, or assumes any legal liability or responsibility for the accuracy, completeness, or usefulness of any information, apparatus, product, or process disclosed, or represents that its use would not infringe privately owned rights. Reference herein to any specific commercial product, process, or service by trade name, trademark, manufacturer, or otherwise does not necessarily constitute or imply its endorsement, recommendation, or favoring by the United States Government or any agency thereof. The views and opinions of authors expressed herein do not necessarily state or reflect those of the United States Government or any agency thereof.

The submitted manuscript has been authored by a contractor of the U. S. Government under contract No. W-31-109-ENG-38. Accordingly, the U. S. Government retains a nonexclusive, royalty-free license to publish or reproduce the published form of this contribution, or allow others to do so, for U. S. Government purposes.

For presentation at the 1995 ASME/STLE Tribology Conference, Kissimmee, FL, October 8-11, 1995

\*Work supported by the U.S. Department of Energy, under Contract W-31-109-Eng-38.

+Permanent address: Sakarya University, Department of Metallurgical Engineering, Adapazari-Turkey.

DISTRIBUTION OF THIS DOCUMENT IS UNLIMITED 85  
**MASTER**

**DISCLAIMER**

**Portions of this document may be illegible in electronic image products. Images are produced from the best available original document.**

## TRIBOLOGICAL PROPERTIES OF HARD CARBON FILMS ON ZIRCONIA CERAMICS

Ali Erdemir (Member, STLE), Cuma Bindal, and George R. Fenske  
Tribology Section  
Energy Technology Division  
Argonne National Laboratory, Argonne, IL 60439

Paul Wilbur  
Department of Mechanical Engineering  
Colorado State University  
Fort Collins, CO 80523

### ABSTRACT

In this study, we investigated the tribological properties of hard diamondlike carbon (DLC) films on magnesia-partially-stabilized zirconia (MgO-PSZ) substrates over a wide range of loads, speeds, temperatures, and counterface materials. The films were 2  $\mu\text{m}$ -thick and produced on by ion-beam deposition at room temperature. Tribological tests were conducted on a ball-on-disk machine in open air of 30 to 50% relative humidity under contact loads of 1 to 50 N, at sliding velocities of 0.1 to 6 m/s, and at temperatures to 400°C.  $\text{Al}_2\text{O}_3$  and  $\text{Si}_3\text{N}_4$  balls were also used and rubbed against the DLC-coated MgO-PSZ disks, primarily to assess and compare their friction and wear performance to that of MgO-PSZ balls. A series of long-duration lifetime tests was run at speeds of 1, 2, and 6 m/s under a 5-N load to assess the durability of these DLC films. Test results showed that the friction coefficients of MgO-PSZ balls sliding against MgO-PSZ disks were in the range of 0.5-0.8, and the average specific wear rates of MgO-PSZ balls ranged from  $10^{-5}$  to  $5 \times 10^{-4}$   $\text{mm}^3/\text{N}\cdot\text{m}$ , depending on sliding velocity, contact load and ambient temperature. The friction coefficients of MgO-PSZ balls sliding against the DLC-coated-MgO-PSZ disks varied between 0.03 to 0.1. The average specific wear rates of MgO-PSZ balls were reduced by factors of three to four orders of magnitude when rubbed against the DLC coated disks. These DLC films could last 1.5 million to 4 million cycles, depending on sliding velocity. Scanning electron microscopy and micro-laser Raman Spectroscopy were used to elucidate the microstructural and chemical nature of DLC films and worn surfaces.

## INTRODUCTION

Hard diamond-like carbon (DLC) or amorphous carbon films combine unusual mechanical and chemical properties that make them very attractive for a wide range of engineering applications [1-4]. Mechanically, these films are very hard and resilient. Reported hardness values for DLC range from 2000 to 9000 kg/mm<sup>2</sup> [1-4,5,6]. Chemically, they are inert and impervious to acidic and saline media. Electronically, they are insulating and optically they can be made transparent to visible and ultraviolet lights [1,2,4,7,8].

Compared to hard nitride and carbide coatings, the DLC coatings can be deposited at temperatures ranging from sub-zero to 300°C and at fairly high deposition rates by a variety of methods including; ion-beam deposition, DC and RF sputtering, arc-plasma, and plasma enhanced chemical vapor deposition, laser ablation [1-4,9-13]. Depending on the deposition method and carbon source, large amounts of hydrogen (e.g., 10-50 at.%) may be present within the structure of DLC films [1,5,13]. Structurally, the DLC films are amorphous. Accordingly, they are sometimes referred to as hydrogenated amorphous carbon films. Within the amorphous structure of DLC very-short-range-ordered diamond (characterized by sp<sup>3</sup>-type tetrahedral bonds) and graphitic phases (characterized by sp<sup>2</sup>-type trigonal bonds) also exist [1,5,13]. Hence, these films can be regarded as degenerate forms of bulk diamond and/or graphite.

Adding to their unique mechanical, chemical, electronics, and optical properties is their unusual capacity to impart very low friction and high wear resistance to sliding tribological interfaces [3,4,7,10,12,14-22]. The sliding friction coefficients of pairs with a DLC coating may range from 0.005 to 0.3, depending on the test conditions, deposition methodology, and counterface materials [7,10,15,18,19]. The relative humidity of the test environment was found to have the greatest effect on the frictional behavior of DLC films. For example, in dry air and inert gases, the friction coefficients of 0.005 to 0.02 are feasible [14,15,18]. However, in humid air, their friction coefficients may go up to ≈0.3 during sliding against

both the metallic and ceramic materials [16,19]. Despite the opportunities and excellent prospects for their use in numerous tribological applications, DLC films have not yet been commercially exploited in large scales.

The primary purpose of this paper is to explore the tribological performance of thin DLC films over a wide range of loads, speeds, and temperatures and to elucidate their chemical and microstructural nature using scanning electron microscopy (SEM) and micro-laser Raman Spectroscopy.

## **EXPERIMENTAL DETAILS**

### **Test Material**

The balls and disks used in this study were made of sintered magnesia-partially-stabilized  $ZrO_2$  (MgO-PSZ). Selected properties of this ceramic are given in Table 1 [23]. The disk specimens, 75 mm in diameter by 6 mm thick, were diamond-wheel ground to a surface finish of  $\approx 0.1 \mu\text{m}$  centerline average (CLA).

The balls were 9.5-mm-diameter and had a surface finish of better than  $0.01 \mu\text{m}$  CLA. They were secured to the ball holder of the wear test machine to assume the vertical ball-on-disk configuration. The balls and the disks were ultrasonically cleaned sequentially in hexane + 10 vol.% toluene, acetone, deionized water containing 2 wt.% laboratory detergent, and deionized water for about 1 min each, then dried in an oven at  $110^\circ\text{C}$  for 20 min. This cleaning sequence was shown in Ref. [24] to remove much of the organic contamination from the exposed surfaces of oxide ceramics.

## **Ion-Beam Deposition of Diamond-Like Carbon**

DLC films used in this study were  $\approx 2 \mu\text{m}$  thick and produced on MgO-PSZ substrates by means of ion-beam deposition in a vacuum chamber equipped with a broad-beam ion source. Figure 1 is a schematic depiction of the ion-beam deposition system. The MgO-PSZ substrates were first positioned beneath the ion source and sputter-cleaned with a 1 keV,  $2.5 \text{ mA/cm}^2$  Ar-ion beam for  $\approx 3\text{-}5$  min. This step was essential for removing adsorbates and/or contaminants from the substrate surface. Next, an intermediate hydrogenated-silicon carbide (SiC:H) bond-layer was sputter-deposited on the substrates by rotating the sample out of the beam and into the sputter-coating position (see Fig. 1). Methane is bled into the vacuum chamber and the 1-keV argon beam is allowed to sputter the silicon target shown in the figure. The combination of the Si being sputtered onto the sample and the C and H derived from the methane gives a SiC:H layer. A 50 nm thick SiC:H layer on MgO-PSZ was found to be sufficient for excellent bonding between MgO-PSZ and DLC films. Finally, the source was switched to methane operation by rotating the substrates back to the position directly beneath the beam. The methane gas (carbon source) was fed through the cylindrical-ion-source and was ionized by energetic-electrons emitted by a hot-filament-wire. The ionized-species pass through a biased grid where they gain a high-acceleration energy of 450 eV a current density of  $\approx 2.5 \text{ mA/cm}^2$ . To overcome charging of the insulating MgO-PSZ substrate, the energetic-ions are neutralized by a hot-filament-wire emitting thermionic electrons. Without discharging, the insulating substrate tends to accumulate positive electrical charge and repels depositing species having the same polarity. The deposition rate was  $\approx 3 \mu\text{m/hr}$ . Substrates were water-cooled via their mounting plates to maintain their temperatures below  $200^\circ\text{C}$  throughout the deposition.

## Friction and Wear Tests

Friction and wear tests were conducted on a ball-on-disk tribometer with the pairs of MgO-PSZ balls and MgO-PSZ disks; and MgO-PSZ balls and DLC-coated MgO-PSZ disks in open air of 30 to 50% relative humidity. A few balls of  $\text{Al}_2\text{O}_3$  and  $\text{Si}_3\text{N}_4$  ceramics were also used and rubbed against the DLC-coated MgO-PSZ disks, primarily to assess and compare their friction and wear behavior to that of MgO-PSZ balls. The normal load applied to the balls ranged from 1 to 50 N, which initially created mean Hertzian contact pressures of approximately 317 MPa to 1.17 GPa, respectively (ignoring any effects of the DLC film). Because of the formation of a flat wear-scar during sliding contacts, nominal bearing pressures fell to a fraction of these initial Hertzian values by the end of the tests. The frictional force was monitored with the aid of a load cell and was recorded on a chart paper throughout the tests. The sliding velocity ranged from 0.1 to 6 m/s during tests evaluating the effects of load and velocity on friction and wear. The sliding distance was 2 km. A series of tests was run to assess the long-term tribological performance and durability of DLC coatings under a 5-N load at velocities ranging from 1 to 6 m/s. The elevated test temperatures, e.g., 100, 200, 300, and 400°C, were created by quartz heaters placed beneath the rotating MgO-PSZ disks.

Wear-volume calculations on the balls were based on microscopic determination of the diameter of the circular wear scars, combined with the assumption that the wear scar is flat [25]. These wear volumes were converted into average specific wear rates by simply normalizing wear volume ( $\text{mm}^3$ ) over contact load (N) and total sliding distance. The wear of disk specimens was assessed from the traces of surface profiles across the wear tracks. Two to three duplicate tests were run under each test condition to check the reproducibility of the friction and wear data and the average values with the spread are reported

## RESULTS

### Film Microstructure and Chemistry

Figure 2 is a cross-sectional SEM micrograph of a DLC coating used in this study. At the magnification shown, this film looks featureless, quite dense, and free of volume defects. The columnar morphology, that is typical of metallic and ceramic coatings produced by physical vapor deposition methods, is not obvious in this DLC coating. The bonding between the DLC coating and the MgO-PSZ substrate appears good and the interface between them is hard to discern.

Figure 3 shows the Raman spectrum of the DLC film. The main features in this spectrum are that there exist two broad peaks; one is positioned at  $\approx 1350 \text{ cm}^{-1}$  (appearing as a shoulder) and the other is centered at  $\approx 1520 \text{ cm}^{-1}$ . The shouldered peak at  $1350 \text{ cm}^{-1}$  may be representing amorphous carbon with an  $\text{sp}^3$ -type bonding, while the broad peak at  $1520 \text{ cm}^{-1}$  may have been due to the graphitic precursors in the DLC film. In general, these peaks are typical of most carbon materials classified as DLC [1,26-28].

### Friction and Wear

#### Effect of Sliding Velocity

Figure 4 shows the friction coefficients and the average specific wear rates of test pairs as a function of sliding velocity. As is evident, the friction coefficients of pairs without a DLC coating are quite high and vary significantly with sliding velocity (see Fig. 4a). Up to 1 m/s, their friction coefficients range from 0.7 to 0.8. However, they decrease substantially with increasing velocity. At 6 m/s, the friction coefficients of pairs without a DLC coating are  $\approx 0.5$ . The friction coefficients of pairs with a DLC



coating vary between 0.07 and 0.1 and they are relatively insensitive to increasing velocity.

The average specific wear rates of MgO-PSZ balls sliding against the uncoated and DLC-coated MgO-PSZ disks are shown in Fig. 4b. Depending on velocity, their wear rates vary between  $\approx 10^{-4}$  to  $\approx 10^{-5}$   $\text{mm}^3/\text{N.m}$  during sliding against the uncoated disks. Whereas, the wear rates of those balls sliding against the DLC-coated disks are  $5 \times 10^{-9}$  to  $10^{-8}$   $\text{mm}^3/\text{N.m}$ . Note that these values are 3 to 4 orders of magnitude lower than the wear rates of balls slid against the uncoated disks. Photomicrographs in Fig. 5 compare the actual size and appearance of two scars formed on MgO-PSZ balls during tests at 1 m/s. As is clear, the size of a wear scar formed on a ball slid against the uncoated MgO-PSZ disk (Fig. 5a) is much greater than that of the wear scar formed during sliding against a DLC-coated MgO-PSZ (Fig. 5b) disks.

SEM microscopy of the worn surfaces of balls and uncoated-disk revealed that plastic flow, microcutting, and microfracture were the dominant modes of wear. At high velocities (e.g., 2 m/s and up), wear was largely dominated by thermal and/or thermomechanical cracking of sliding surfaces (Fig. 6a). At 6 m/s, even some evidence of local melting was noticed (Figs. 6b and c). Fig. 6b is taken from the middle of a wear scar and provides evidence for extensive thermomechanical cracks and local melting. Wear-debris particles found on and around the wear scar consisted of large fragments which may have been produced by local melting of asperity tips and/or fine debris particles trapped at these interfaces sliding at high velocities (Fig. 6c).

3-D surface maps in Fig. 7 compare the extent of wear on an uncoated-disk with that on a DLC-coated MgO-PSZ disk after wear tests under identical conditions. The extent of wear on uncoated disk is rather significant and the width of wear track is quite large, but the wear of DLC-coated disk is hard to discern. Using a surface profilometer at vertical magnifications up to 50,000X, we were unable to detect any

measurable wear losses on this disk. Further examinations with SEM revealed that the wear was essentially confined to the sharp tips of surface asperities but the DLC coating itself was still intact after the 2 km long sliding tests.

### **Effect of Load**

Figure 8 shows the effect of increasing load on the friction coefficients and the average specific wear rates of the MgO-PSZ balls during sliding against the DLC-coated MgO-PSZ disks. As is clear, the friction coefficients of test pairs decreased with increasing load (see Fig. 8a). At a 1-N load, the friction coefficient is  $\approx 0.09$ , but decreased monotonically with increasing load. At a 50-N load, it was  $\approx 0.03$ .

Fig. 8b shows the effect of load on the average specific wear rates of MgO-PSZ balls slid against the DLC-coated MgO-PSZ disks. Except at a 1-N load, the average specific wear rate of balls was relatively high under lower loads (e.g.,  $\approx 5 \times 10^{-9}$  mm<sup>3</sup>/N.m under a 2-N load). However, it decreased substantially with increasing load. For instance, at a 20-N load, the average specific wear rate was by an order of magnitude lower than that at a 2-N load. When load is further increased to 50 N, the wear rate remained essentially the same. Note that the values in brackets and parantheses given along the data points in Fig. 8b indicate the mean initial Hertzian and final nominal contact pressures (in GPa), respectively, that develop between ball and disk specimens.

### **Effect of Ambient Temperature**

Figure 9 shows the effect of test temperature on friction and wear performance of MgO-PSZ pairs with and without a DLC coating. As is evident from Fig. 9a, the friction coefficients of pairs without a DLC coating was  $\approx 0.75$  at room temperature but increased to  $\approx 0.82$  when temperature was raised to 200°C.

A slight decrease was seen during tests at 300°C. However, for those pairs with a DLC coating, the friction coefficients were in the range of 0.07 to 0.1 at room temperature, but decreased to  $\approx 0.05$  when temperature was raised to 200°C. At 300°C, their friction coefficients increased slightly to  $\approx 0.08$ .

As shown in Fig. 9b, the average specific wear rates of MgO-PSZ balls sliding against the uncoated MgO-PSZ disks decreased significantly when temperature was raised to 100°C. However, upon further increasing the temperature to 200 and 300°C, the average specific wear rates remained relatively unchanged. As for the balls sliding against the DLC-coated disks, their average specific wear rates decreased slightly when temperature was raised to 100°C, but increased substantially as temperature was further raised to 200 and 300°C. Attempts were made to perform friction tests on DLC-coated disks at 400°C, however, by the time temperature reached and stabilized at 400°C, it was noticed that much of the DLC coating had flaked out and the underlying substrate was partially exposed as verified by SEM and X-ray mapping in Fig. 10. Consequently, no tests were run at 400°C.

Microscopic examination of the sliding contact surfaces revealed that there was significant amount of wear on both the balls and the uncoated disks. Whereas, the extent of wear on DLC-coated disks and on balls slid against these disks was rather insignificant even after tests at 300°C. 3-D surface maps in Figs. 11a and 11b show qualitatively the extent of wear damage on an uncoated and a DLC-coated MgO-PSZ disks, respectively, after wear tests at 300°C.

#### **Effect of Counterface Material**

Figure 12 compares the friction coefficients and the average specific wear rates of  $\text{Al}_2\text{O}_3$ ,  $\text{Si}_3\text{N}_4$ , and MgO-PSZ balls sliding against DLC-coated MgO-PSZ disks. The variation of friction coefficients from one ball to another is not substantial e.g., 0.07 to 0.09; however, the variation of average specific wear

rates is quite significant. For instance, the wear rate of  $\text{Al}_2\text{O}_3$  balls was by a factor of 4 lower than that of MgO-PSZ balls. It was interesting to note that there existed no correlation between friction coefficients and average specific wear rates of the pairs shown in Fig. 12. The  $\text{Al}_2\text{O}_3$  balls exhibited the highest friction coefficient yet the lowest wear of all during sliding against the DLC coatings.

### **Lifetime of DLC Coatings**

Figure 13 and accompanying table present the friction and wear performance of DLC-coatings subjected to lifetime tests at velocities of 1, 2, and 6 m/s. As is evident, in all cases, these coatings possessed endurance lives of millions of sliding cycles. Initially, the friction coefficients of these DLC coatings sliding against the MgO-PSZ balls were on the order of 0.1 (this region is denoted with letter A in Fig. 13), but decreased steadily with increasing number of sliding cycles and eventually reached values of 0.05 to 0.06 (this region is denoted with letter B). After millions of sliding passes, the friction coefficients began to increase as the DLC coatings wore out (point C in Fig 13). With further sliding, the film was worn out, friction tended to increase, and the substrate MgO-PSZ became exposed (this point is denoted with letter D in Fig. 13). The increase in friction is thought to be due to the fact that the balls were partially sliding against the exposed substrate. From the data in accompanying table, it is clear that the lifetimes of DLC coatings are influenced significantly by the sliding velocity. In general, the higher the sliding velocity the lower the lifetimes of DLC coatings.

The average specific wear rates of the counterface balls were  $3.3 \times 10^{-8}$  to  $7 \times 10^{-9}$   $\text{mm}^3/\text{N.m}$ . Figure 14 shows the 3-D surface maps of typical wear tracks formed on a DLC-coated MgO-PSZ disk after lifetime tests at 1 and 6 m/s.

## DISCUSSION

From the results presented above, it is clear that without a DLC coating, the balls and disks suffer heavy wear damage. Increasing velocity has a significant effect on the friction and wear behavior of MgO-PSZ material. The DLC coatings impart very low friction and wear losses to sliding MgO-PSZ interfaces over the range of sliding velocities, contact loads, and ambient temperatures explored in this study.

### Friction and Wear

Generally poor wear performance of MgO-PSZ material (see Figs. 4b, 5a, 9) can be attributed to their poor thermal shock resistance and inherent brittleness. Because of a very poor thermal conductivity (e.g., at 293 K,  $k_{\text{MgO-PSZ}} = 3.08 \text{ W/m.K}$ ), the MgO-PSZ cannot effectively dissipate frictional heat generating at high sliding velocities. Virtually, all the mechanical work done to overcome friction between MgO-PSZ balls and disks is released as heat, and this heat is primarily confined to the areas of real contact spots. These spots are sometimes referred as "hot spots". Large temperature gradients can easily develop between the hot spots and surrounding regions; these in turn create high thermal stresses. When these stresses are combined with the high normal and tangential stresses, microcracks (Figs. 6a and b) may develop and promote wear [29]. Temperature and/or stress-induced phase transformation is also feasible in zirconia-base ceramics and may have contributed to their high wear rates.

When sliding velocity is very high, e.g., 6 m/s, the magnitude of frictional heat generating at hot spots may become so high that local melting become feasible. The micrographs in Figs. 6b and c of this study reveal some microfeatures indicative of local melting. In fact, Fig. 6b suggests that melt volume at sliding interface could easily be smeared on the surface to form a bridge over a thermal crack. Some of the melt volume can be squeezed out of the sliding interface and solidifies around the trailing edges of the balls. The solidified portions can then be chipped away by dynamic sliding, thus becoming large wear

fragments as shown in Fig. 6c.

In addition to the thermal cracks and local asperity melting, tensile cracks may also develop at sliding interfaces of balls and disks and promote wear. As reported by Hamilton and Goodman [30], when friction coefficient exceeds 0.3, the maximum shear stress moves from the subsurface toward the sliding surfaces. The tensile component of shear stress is developed behind the sliding asperities and the higher the friction coefficients, the greater the magnitude of the tensile forces. As shown in Figs. 4a and 9a, the steady-state friction coefficients of the MgO-PSZ test pairs are quite high during tests at high sliding velocities and temperatures. Under the test conditions explored in this study, maximum shear stresses must have been at the plane of sliding interfaces and that large tensile forces must have generated behind the moving asperities. As a result, some contact areas on sliding surfaces suffered wear due to microfracture.

#### **Test Pairs With DLC Films**

The results presented in Figs. 4, 8, 9, 12, and 13 demonstrate that the DLC coatings used in this study can impart very low friction coefficients and high wear resistance to sliding MgO-PSZ surfaces over a wide range of velocities and contact loads. Furthermore, these coatings can last over millions of stress cycles even at very high sliding velocities. We believe that strong adhesion provided by the SiC:H bondlayer was primarily responsible for the excellent durability and load-bearing capacity of DLC coatings. Without strong bonding, DLC coatings would have been easily removed from the surface of MgO-PSZ substrate under the influence of dynamic sliding and very high contact stresses.

Despite their excellent durability and load-bearing capacity at room temperature, these DLC coatings delaminated at high temperatures, (e.g.,  $>300^{\circ}\text{C}$  in air) and left their substrates partially unprotected (see Fig. 10). Therefore, the tribological use of these coatings in open air should be confined to temperatures

below 300°C.

The absence of tensile cracks and local asperity melting on the surfaces of MgO-PSZ balls slid against the DLC-coated disks can be attributed to the relatively low friction coefficients of these surfaces against DLC coating. Because, lower the friction coefficients, the lower the magnitude of tensile forces and that of flash heating. As is evident from Fig. 5b, those balls slid against a DLC-coated MgO-PSZ disk experienced very little wear.

The exceptional wear resistance of DLC coatings is primarily attributed to their high mechanical strength and hardness (e.g, 2000 to 9000 kg/mm<sup>2</sup>) [14-22]. However, their low friction nature has not yet been well-understood. It has been speculated that their high chemical inertness may have been largely responsible for their low friction characters, but other mechanisms such as micro-graphitization [9,33-37] and the formation of transfer-layers [16,19-22] on mating surfaces have also been proposed. It is important to remind that most of these hypotheses are based on observations made on a specific DLC film tested under very specific test conditions. The family of DLC coatings is rather large. Depending on the deposition method and/or condition, graphitelike phases and large amounts of hydrogen may be present in their structures. Therefore, the proposed friction mechanisms should not be regarded as universal and applicable to all carbon films designated as DLC.

From a tribological stand point, one can argue that the extent of friction between two sliding surfaces is an interplay between the physicochemical nature of the microcontact interfaces, contact stresses, and surrounding environment. Physically, rougher surfaces can cause increased ploughing, hence higher friction. Whereas, the chemical interactions between the sliding surfaces govern the extent of adhesive bonding across the sliding interface. In the presence of a soft metal or lamellar solid lubricant at a sliding interface, low friction is largely attributed to the easy shear character of these solids. However, with their high mechanical strength and rigidity, DLC coatings cannot shear easily, hence similar mechanisms

cannot be used here to explain their low friction character. We believe that the generally low friction coefficients of MgO-PSZ balls sliding against the DLC films of this study are primarily due to the highly inert nature of these films. Furthermore, the formation of a carbon-rich transfer layer on counterface balls is responsible for their excellent endurance lives and much reduced friction coefficients observed during lifetime tests.

As reported by a number of researchers [31-36], active species like hydrogen, oxygen or water vapor can attach and passivate the dangling surface bonds of most carbon materials including diamond and graphite. Apparently, when these dangling bonds are passivated, adhesion component of friction is drastically reduced. In fact, the low-friction character of diamond is largely attributed to the highly passive nature of its sliding surface [33-35]. When hydrogen and other species are desorbed or removed from the sliding surfaces of diamond and/or graphite (e.g., by ion-beam sputtering and/or high-temperature annealing in vacuum), friction coefficient increases drastically, presumably because of the reactivated dangling bonds causing strong adhesive interactions between diamond and counterface ball material [31, 33-36]. Most DLC films contain high proportions of hydrogen in their structures. So, they are inherently saturated with a specie that passifies dangling bonds of carbon precursor causing high adhesive interactions. In a number of recent studies [7,16,37, 38], it was demonstrated that the friction coefficients of DLC films sliding against steel balls could also increase substantially if hydrogen was desorbed from their bulks by annealing in high-vacuum. Thus, just like diamond, the low friction character of DLC films too can be attributed to the pasivation of dangling bonds making their surface very inert and insensitive.

**Friction and Wear Against Other Ceramics:** Variations in friction and wear performance of DLC coatings against various ceramic balls can be attributed to the inherently different physical, chemical, and mechanical properties of each ceramic ball. The extent of friction between two sliding surfaces is known



to be controlled largely by surface mechanical, physical, and chemical interactions. It is thought that with different, mechanical, physical, and chemical states, each ball surface will have different degrees of interaction with DLC surfaces, hence the slight variations in their friction coefficients against DLC surfaces should not be regarded as unusual. As for the large differences in wear, it is believed that mechanical and thermal properties of sliding balls play the major roles. Much higher wear factor of MgO-PSZ balls can be attributed to their relatively lower hardness and poorer thermal conductivities than the other balls. Overall, the friction and wear performance of all ceramic balls should be considered quite good considering the severe sliding conditions created during each test.

## SUMMARY

In general, hard DLC films used in this study afforded excellent friction and wear properties to sliding MgO-PSZ interfaces over a wide range of pressures, velocities and temperatures. Test results showed that without the DLC coatings, the sliding pairs of MgO-PSZ experienced high friction and wear losses, especially at high sliding velocities where thermal and/or thermomechanical instabilities become more pronounced. Inherently low thermal shock resistance and poor thermal conductivity of this ceramic were particularly detrimental to their generally poor wear performance. The friction and wear data suggested that, without proper lubrication, MgO-PSZ ceramics should not be considered for demanding tribological applications. The DLC coatings were very effective in reducing friction and wear of sliding surfaces of MgO-PSZ material. They reduced friction coefficients of test pairs by factors of 8 to 20 and the average specific wear rates of balls by factors of three to four orders of magnitude, depending on contact load, velocity, and ambient temperature. Moreover, these DLC films could last 1.5 million to 4 million cycles, depending on sliding velocity. Strong film-to-substrate adhesion afforded by a 50 nm thick SiC:H bond layer was essential for such long endurance lives. The exceptional friction and wear properties of DLC films are attributed to their high chemical inertness and mechanical hardness. Ion-beam deposition process used in this study was quite capable of producing high-quality amorphous DLC

films on MgO-PSZ substrates.

## ACKNOWLEDGEMENT

The authors wish to thank C. Zuiker of Argonne National Laboratory for performing the laser-Raman spectroscopy. This work was supported by the U.S. Department of Energy under Contract W-31-109-Eng-38.

## REFERENCES

1. Tsai, H. and Bogy, D. B., "Characterization of Diamondlike Carbon Films and Their Application as Overcoats on Thin-Film Media for Magnetic Recording," *J. Vac. Sci. Technol.*, A5 (1987) pp. 3287-3312.
2. Grill, A., Patel, V., and Meyerson, B. S., "Applications of Diamond-like Carbon in Computer Technology," in *Applications of Diamond Films and Related Materials* (Y. Tzeng, M. Yoshikawa, A. Feldman, Eds.) Elsevier Science, Publishers, B.V., 1991, pp.683-689.
3. Braza, J. F., and Sudarshan, T. S., "Tribological Behavior of Diamond and Diamondlike Carbon Films: Status and Prospects," in *Surface Modification Technologies V*, (T. S. Sudarshan and J. F. Braza, eds.), The Institute of Materials, 1992, pp. 801-819.
4. "Status and Applications of Diamond and Diamond-like Materials: An Emerging Technology," National Materials Advisory Board, Washington D.C., (1990)

5. Robertson, J., "Amorphous Carbon," *Advan. Phys.*, 35(1986), pp. 317-374.
6. Mirtich, M. J., Swec, D. M., and Angus, J. C., "Dual Ion Beam Deposition of Carbon Films with Diamondlike Properties, NASA Tech. Mem. 83743, Nasa Lewis Research Center, 1984.
7. Grill, A., Patel, V., and Meyerson, B. S., "Optical and Tribological Properties of Heat-treated Diamond-like Carbon," *J. Mater. Res.*, 5 (1990) pp. 2531-2537.
8. Enke, K., "Some New Results on the Fabrication and the Mechanical, Electrical, and Optical Properties of i-Carbon Layers," *Thin Solid Films*, 80(1981) 277-234.
9. Cuomo, J. J., Doyle, J. P., Bruley, J., and Liu, J. C., "Sputter Deposition of Dense Diamond-like Carbon Films at Low Temperature," *Appl. Phys. Lett.*, 58, 1991, pp. 1-3.
10. Wei, R., Wilbur, P. J., Erdemir, A., Kustas, F. M., "The Effects of Beam Energy and Substrate Temperature on the Tribological Properties of Hard-carbon Films on Alumina," *Surf. Coat. Technol.*, 51, 1992, pp. 139-145.
11. C. Weissmantel, K. Bewilogua, K. Breuer, D. Dietrich, U. Ebersbach, H.-J. Erlen, B. Rau, and G. Reisse, "Preparation and Properties of Hard i-C and i-BN Coatings," *Thin Solid Films*, 96 (1982) 31-44.
12. Miyoshi, K., Pouch, J. J., and Alterovitz, S. A., "Plasma-Deposited Amorphous Hydrogenated Carbon Films and Their Tribological Properties," *Mater. Sci. Forum*, 52/53 (1989) 645-656.
13. Tanaka, K., Okada, M., Kohno, T., Yanokura, M., Aratani, M., "Hydrogen Content and Bonding Structure of Diamondlike Carbon Films Deposited by Ion Beam Deposition," *Nucl. Inst. Meth. B58*, 1991, pp. 34-38.

14. Enke, K., Dimigen, H., and Hubsch, H., "Frictional Properties of Diamondlike Carbon Layers," *Appl. Phys. Lett.*, 36(1980)291-292.
15. Memming, R., Tolle, H. J., and Wierenga, P. E., "Properties of Polymeric Layers of Hydrogenated Amorphous Carbon Produced by a Plasma-Activated Chemical Vapor Deposition Proces. II Tribological and Mechanical Properties," *Thin Solid Films*, 143(1986)31-41.
16. Erdemir, A., Switala, M., Wei, R., and Wilbur, P., "A Tribological Investigation of the Graphite-to-Diamondlike Behavior of Amorphous Carbon Films Ion Beam Deposited on Ceramic Substrates," *Surface Coatings and Technology*, Volume 50 (1991) pp. 17-23.
17. Erdemir, A., Nichols, F. A., Pan, X. Z., Wei, R., and Wilbur, P., "Friction and Wear Performance of Ion-beam-deposited Diamondlike Carbon Films on Steel Substrates," *Diamond and Rel. Mat.*, 3(1993) 119-125.
18. Miyoshi, K., "Tribological Studies of Amorphous Hydrogenated Carbon Films in a Vacuum, Spacelike Environment," *Applications of Diamond Films and Related Materials*, (Y. Tzeng, M. Yoshikawa, M. Murakawa, A. Feldman, eds.) Elsevier Science, Publ., B.V., 1991, pp. 699-702.
19. Kim, D. S., Fischer, T. E., and Gallois, B., "The Effects of Oxygen and Humidity on Friction and Wear of Diamondlike Carbon Films," *Surf. Coat. Technol.*, 49(1991), pp. 537-542.
20. Hirvonen, J.-P., Koskinen, J., Anttila, A., Lappalainen, R., Toivanen, R. O., Arminen, E., and Trkula, M., "Characterization and Unlubricated Sliding of Ion-Beam-Deposited Hydrogen-free Diamondlike Carbon Films," *Wear*, 141, 1990, pp. 45-58.

21. Hirvonen, J. P., Lappalainen, R., Koskinen, J., Anttilla, A., Jervis, T. R., and Trkula, M., "Tribological Characteristics of Diamond-like Films Deposited with an Arc-discharge Method," *J. Mater. Res.*, 5(1990), pp. 2524-2530.
22. Klafke, D., Wasche, R., and Czichos, H., "Wear Behaviour of i-Carbon Coatings," *Wear*, 153, 1992, pp. 149-162
23. Materials Data Sheet, Nilcra Ceramics Pty., Ltd., Victoria, Australia.
24. Gates, R. S., Yellets, J. P., Deckman, D. E., and Hsu, S. M., "Considerations in Ceramic Friction and Wear Measurements," *Selection and Use of Wear Tests for Ceramics*, ASTM, Philadelphia, STP 1010, Eds. Yust, C. S., and Bayer, R. G., pp. 1-23, (1988).
25. 1990 Annual Book of ASTM Standards, Vol. 3., Wear and Erosion; Metal Corrosion, G99-90, "Standard Test Method for Wear Testing with a Pin-On-Disk Apparatus," ASTM, Philadelphia, PA, 1990, pp. 391-395.
26. Knight, D. S., and White, W. B., "Characterization of Diamond Films by Raman Spectroscopy," *J. Mater. Res.*, 4(1989) pp. 385-393.
27. C. V. Cooper, C.V., Beetz, C. P., Buchholtz, B. W., Wilbur, P., and Wei, R., "Spectroscopic and Selected Mechanical Properties of Diamond-Like Carbon Films Synthesized by Broad-Beam Ion Deposition From Methane", *Surf. Coat. Technol.*, 68/69 (1994) 534-541.
28. Tamor, M. A., and Vassell, W. C., "Raman "Fingerprinting" of Amorphous Carbon Films", *J. Appl.*

Phys., 76(1994) 3823-3830.

29. Winer, W. O., and Ting, B. Y., Development of a Theory of Wear of Ceramics, Final Report to Oak Ridge National Laboratory, ORNL/84-7802/1, Oak Ridge, TN 1988.

30. Hamilton, G. M., and Goodman, L. E., "The Stress Field Created by a Circular Sliding Contact," J. Appl. Mech., Ser. E, 33, pp 371-376 (1966).

31. S. V. Pepper, "Effect of Electronic Structure of the Diamond Surface on the Strength of the Diamond-metal Interfaces," J. Vac. Sci. Technol., 20 (1982) 643-646.

32. Pepper, S. V., "Transformation of the Diamond (110) Surface, J. Vac. Sci. Technol., 20, (1982), pp. 213-217.

33. F. P. Bowden and J. E. Young, Proc. Roy. Soc. London, "Friction of Diamond, Graphite, and Carbon and the Influence of Surface Films," 208 (1951) 444-455.

34. Bowden, F. P., Hanwell, A. E., "The Friction of Clean Crystal Surfaces," Proc. Roy. Soc., A295, 1966, pp. 233-243.

35. Gardos, M. N., and Soriano, B. L., "The Effect of Environment on the Tribological Properties of Polycrystalline Diamond Films," J. Mater. Res., 5, 1990, pp. 2599-2609.

36. Zaidi, H., Mezin, A., Nivoit, A., and Lepage, J., "The Influence of The Environment on The Friction and Wear of Graphitic Carbon", App. Surf. Sci., 40 (1989) 103-114.

37. Grill, A., Patel, V., and Meyerson, B., "Tribological Behaviour of Diamond-Like Carbon: Effects of Preparation Conditions and Annealing", *Surf. Coat. Technol.*, 49 (1991) 530-536.
38. Zaidi, H., Le Huu, L., and Paulmier, D., "Influence of Hydrogen Contained in Hard Carbon Coatings on Their Tribological Behaviour", *Diamond Relat. Mater.*, 3 (1994) 787-790.

Table I. Mechanical and thermal properties of MgO-PSZ

Property	Unit	MgO-PSZ
Hardness (20°C)	GPa	11
Fracture Toughness (20°C)	MPa√m	7.6
(800°C)		5
Young's Modulus (20°C)	GPa	205
Poisson's Ratio (20°C)	-	0.31
Thermal Expansion		
Coefficient (25-800°C)	10 <sup>-6</sup> /°C	10.3
Thermal Conductivity (20°C)	W/m.K	3.08
Bulk density (20°C)	kg/m <sup>3</sup>	5,740
Melting Point	K	2893
Flexural Strength (20°C)	MPa	820
(820°C)		430
Tensile Strength (20°C)	MPa	450
Compressive		
Strength (20°C)	MPa	1990

## FIGURE CAPTION:

Figure 1. Schematic depiction of the ion-beam deposition system.

Figure 2. Cross-sectional SEM micrograph of DLC coating used in this study.

Figure 3. Raman spectrum of DLC coating.

Figure 4. Variation of (a) friction coefficients and (b) average specific wear rates of MgO-PSZ balls during sliding against uncoated and DLC-coated MgO-PSZ disks as a function of sliding velocity (test conditions: load, 5 N; sliding distance, 2 km; relative humidity, 35%; radius of MgO-PSZ balls, 4.77 mm; temperature, 23°C).

Figure 5. SEM micrographs of wear scars of MgO-PSZ balls slid against (a) an uncoated MgO-PSZ disk and (b) a DLC-coated MgO-PSZ disk at 1 m/s (test conditions: load, 5 N; relative humidity, 35%; sliding distance, 2 km; temperature, 23°C; pin radius, 4.77 mm).

Figure 6. Higher magnification SEM micrographs of wear scars formed on MgO-PSZ balls during sliding against uncoated MgO-PSZ disks at (a) 4 m/s and (b) 6 m/s, and (c) large colonies of flakelike wear fragments found around the trailing edges of balls (test conditions: test conditions: load, 5 N; sliding distance, 2 km; relative humidity, 35%; radius of MgO-PSZ balls, 4.77 mm; temperature, 23°C).

Figure 7. 3-D surface maps of wear tracks formed on (a) an uncoated- and (b) a DLC-coated MgO-PSZ disk after wear tests under identical conditions (test conditions: load, 5 N; sliding velocity, 1 m/s; relative humidity, 35%; sliding distance, 2 km; temperature, 23°C; pin radius, 4.77 mm).

Figure 8. Effect of increasing load on (a) friction coefficients and (b) average specific wear rates of the MgO-PSZ balls during sliding against DLC-coated MgO-PSZ disks (test conditions: sliding velocity, 1 m/s; relative humidity, 35%; sliding distance, 2 km; temperature, 23°C; pin radius, 4.77 mm).

Figure 9. Effect of ambient temperature on (a) friction coefficients and (b) average specific wear rates of the MgO-PSZ balls during sliding against uncoated and DLC-coated MgO-PSZ disks (test conditions: load, 5 N; sliding velocity, 1 m/s; relative humidity, 35%; sliding distance, 2 km; pin radius, 4.77 mm).

Figure 10. (a) SEM micrograph and (b) X-ray Zr map of a DLC-coated MgO-PSZ disk after exposure to 400°C test temperature.

Figure 11. 3-D surface maps of wear tracks formed on (a) uncoated and (b) DLC-coated MgO-PSZ disks during sliding against MgO-PSZ balls 300°C (test conditions: load, 5 N; sliding velocity, 1 m/s; relative humidity, 35%; sliding distance, 2 km; pin radius, 4.77 mm).

Figure 12. Friction coefficients and average specific wear rates of  $\text{Al}_2\text{O}_3$ ,  $\text{Si}_3\text{N}_4$ , and MgO-PSZ balls during sliding against DLC-coated MgO-PSZ disks (test conditions: load, 5 N; sliding velocity, 2 m/s; relative humidity, 35%; sliding distance, 2 km; pin radius, 4.77 mm).



Figure 13. Friction and wear performance of DLC-coatings subjected to long-duration sliding tests at velocities of 1, 2, and 6 m/s (test conditions: load, 5 N; relative humidity, 35 to 50 %; pin radius, 4.77 mm; temperature, 23°C).

14. 3-D surface maps of wear tracks formed on DLC-coated MgO-PSZ disks during lifetime tests at (a) 1 m/s and (b) 6 m/s (test conditions: load, 5 N; relative humidity, 35-50%; pin radius, 4.77 mm).

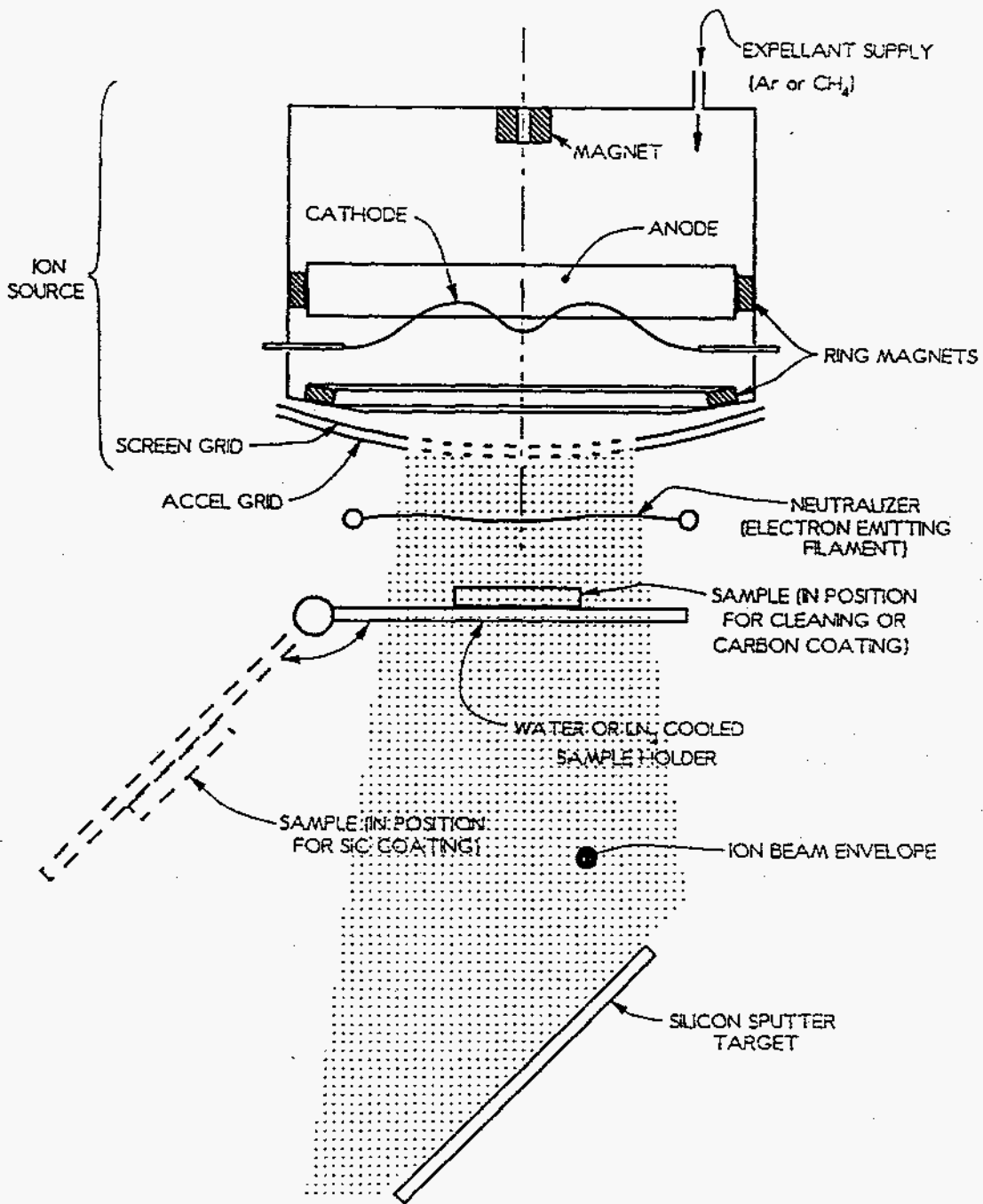


Figure 1. schematic depiction of the ion-beam deposition system.

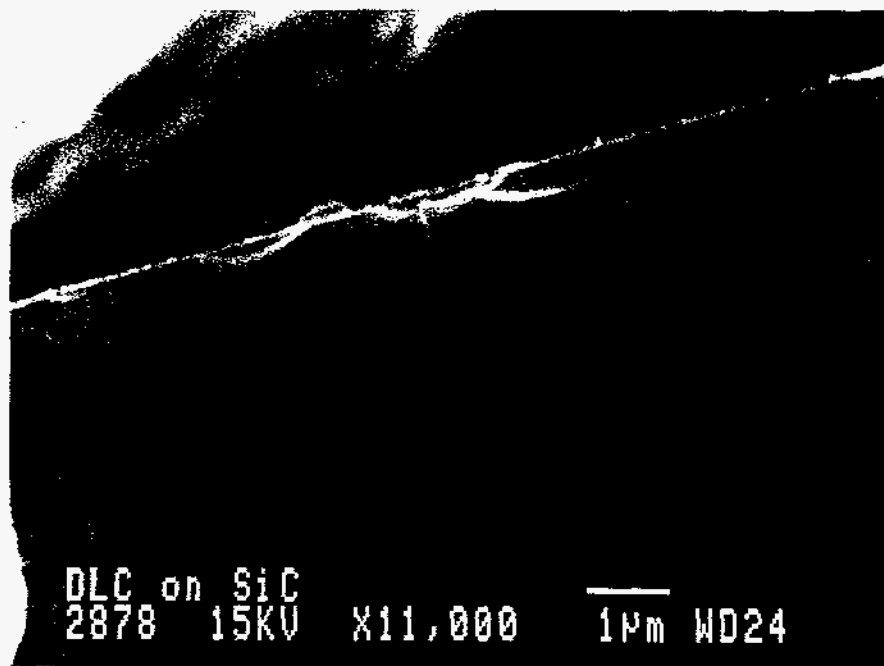


Figure 2. Cross-sectional SEM micrograph of DLC coating used in this study.

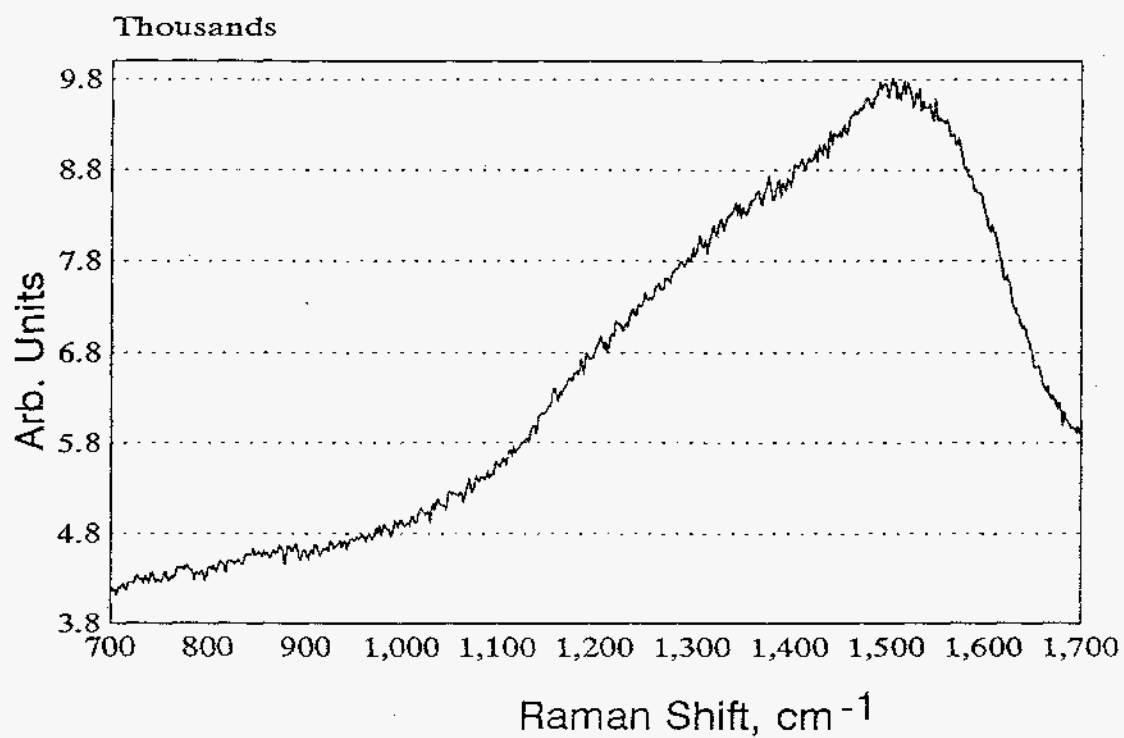
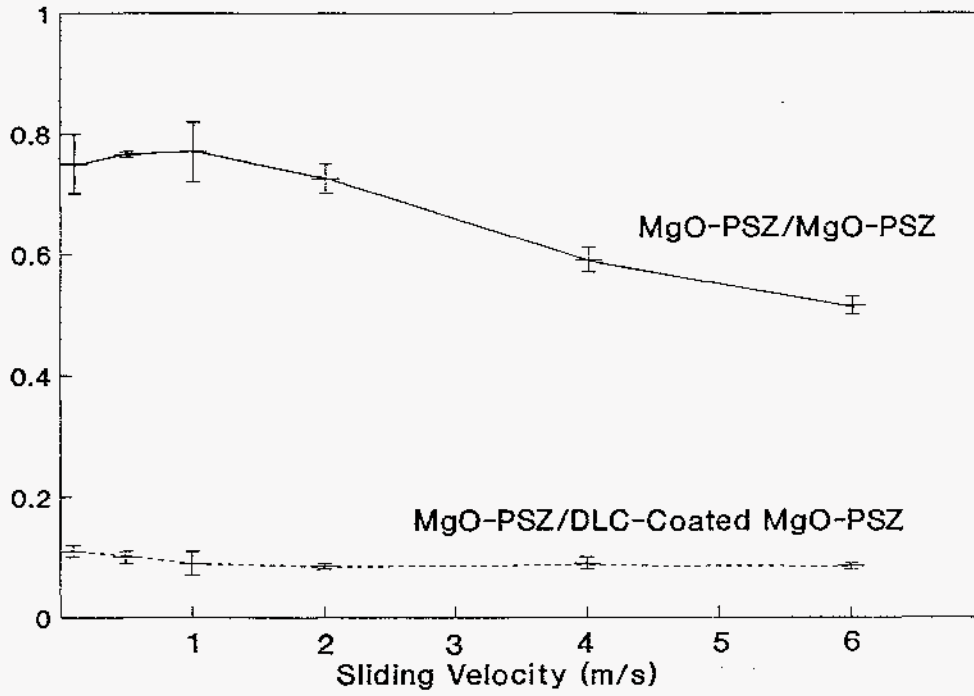
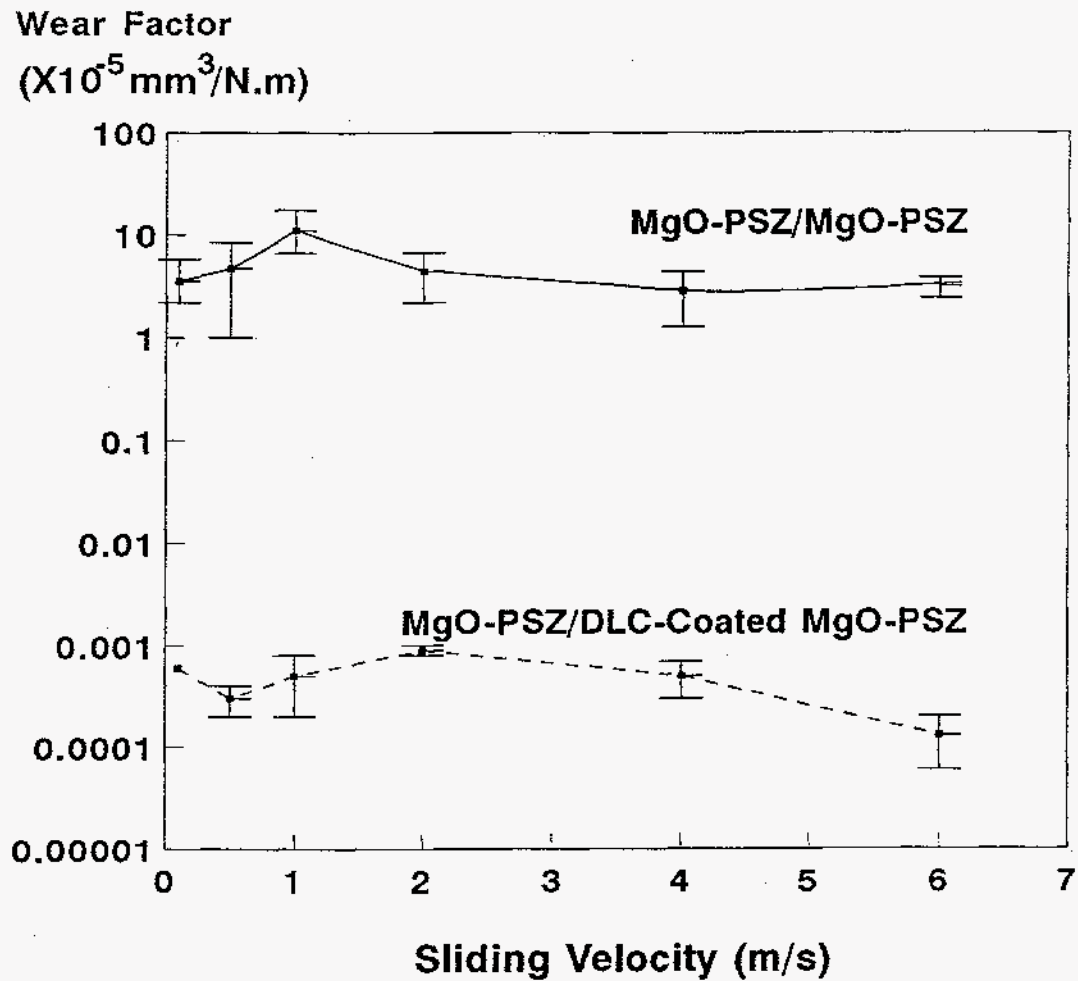


Figure 3. Raman spectrum of DLC coating.

Friction  
Coefficient

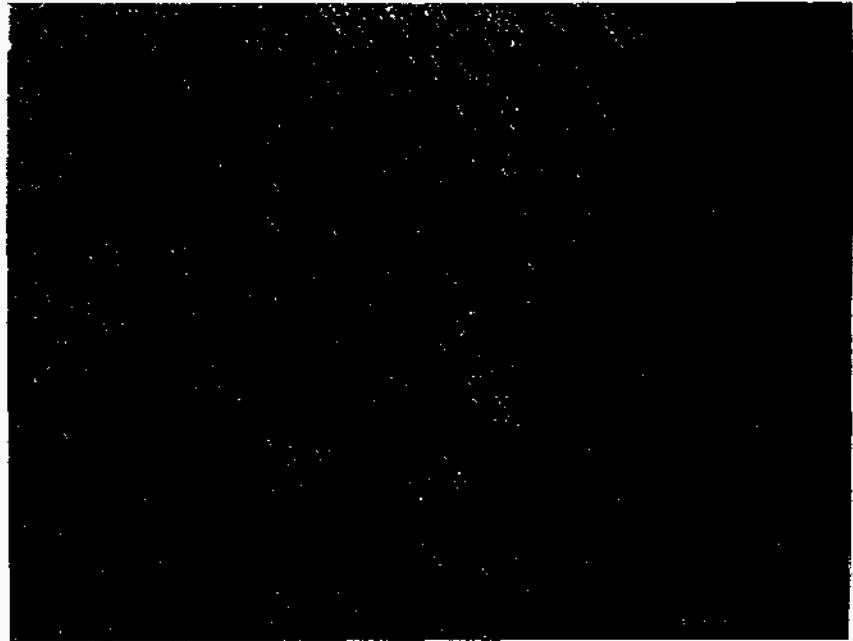


(a)

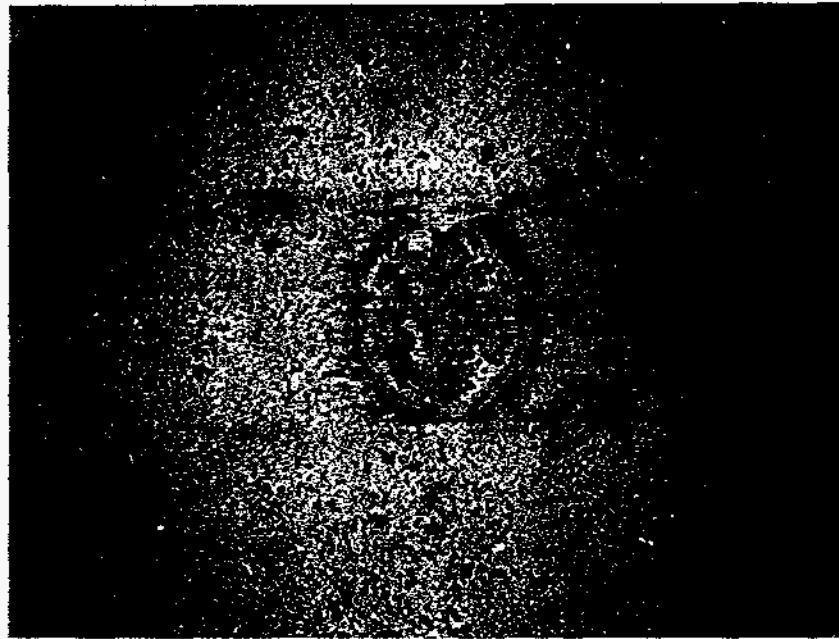


(b)

Figure 4. Variation of (a) friction coefficients and (b) average specific wear rates of MgO-PSZ balls during sliding against uncoated and DLC-coated MgO-PSZ disks as a function of sliding velocity (test conditions: load, 5 N; sliding distance, 2 km; relative humidity, 35%; radius of MgO-PSZ balls, 4.77 mm; temperature, 23°C).

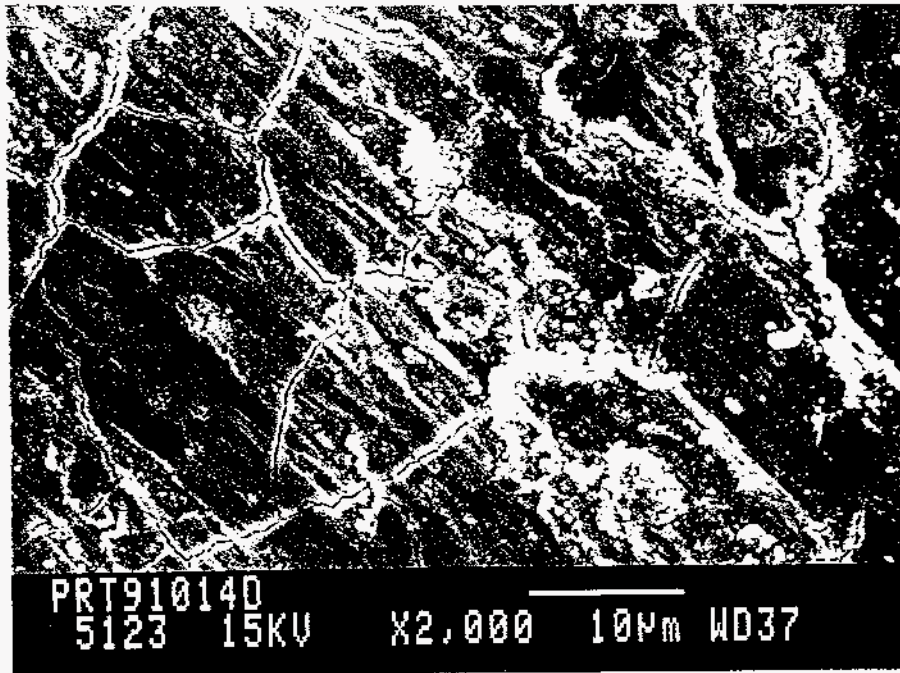


(a) Magnification: 50X



(b) Magnification: 100X

Figure 5. SEM micrographs of wear scars of MgO-PSZ balls slid against (a) an uncoated MgO-PSZ disk and (b) a DLC-coated MgO-PSZ disk at 1 m/s (test conditions: load, 5 N; relative humidity, 35%; sliding distance, 2 km; temperature, 23°C; pin radius, 4.77 mm).



(a)



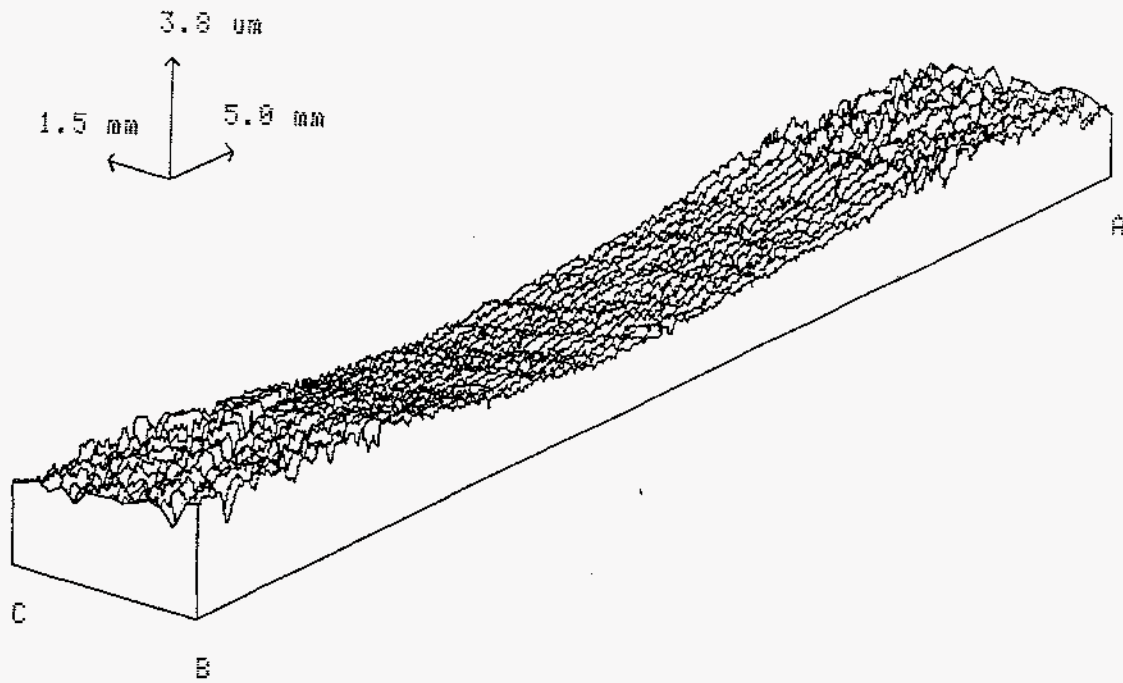
(b)



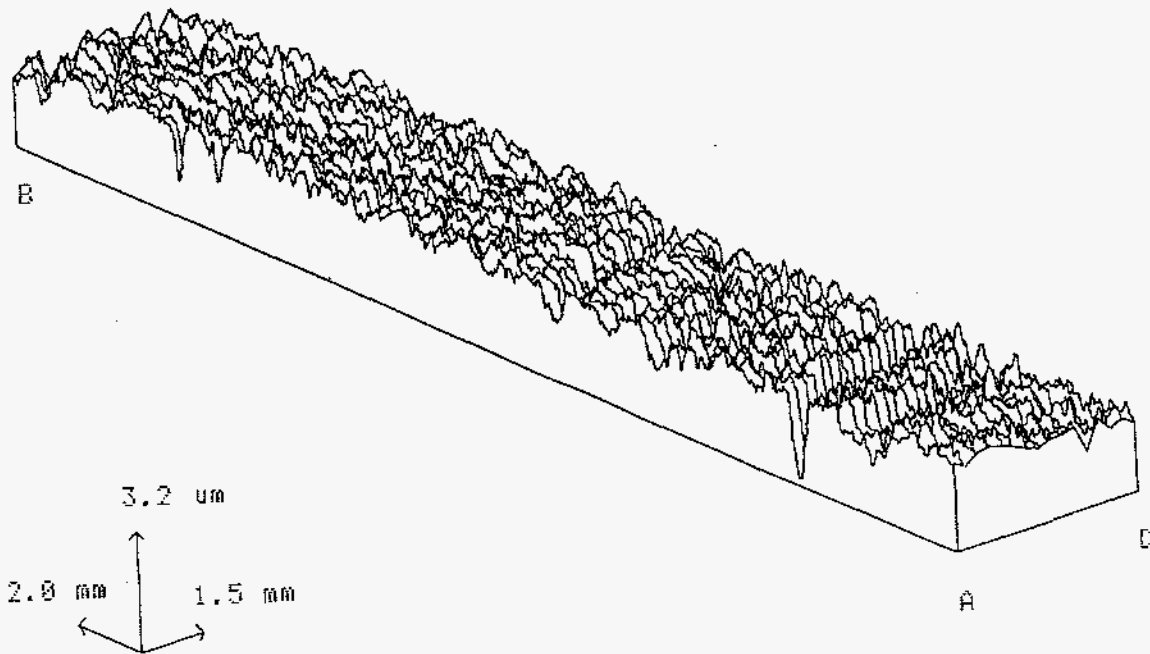
(c)

Figure 6. Higher magnification SEM micrographs of wear scars formed on MgO-PSZ balls during sliding against uncoated MgO-PSZ disks at (a) 2 m/s and (b) 6 m/s, and (c) large colonies of flakelike wear fragments found around the trailing edges of balls (test conditions: test conditions: load, 5 N; sliding distance, 2 km; relative humidity, 35%; radius of MgO-PSZ balls, 4.77 mm; temperature, 23°C).



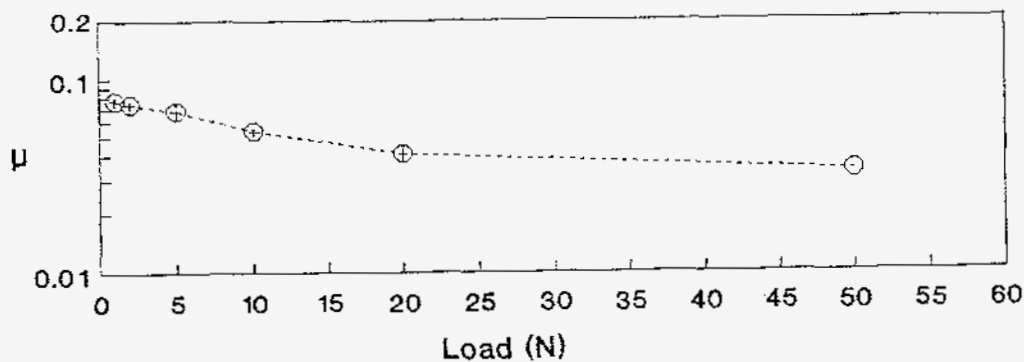


(a)

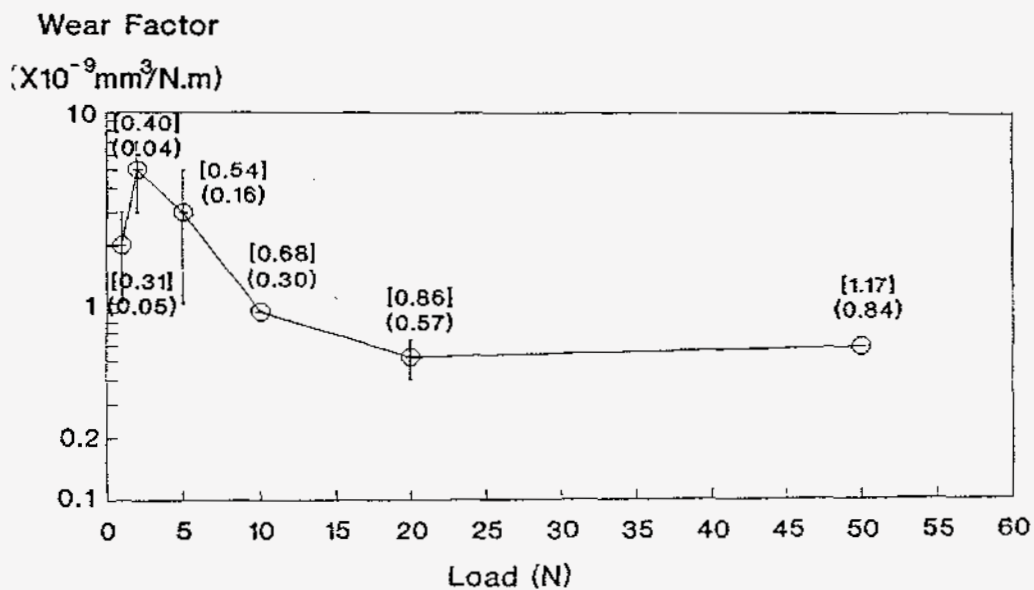


(b)

Figure 7. 3-D surface maps of wear tracks formed on (a) an uncoated- and (b) a DLC-coated MgO-PSZ disk after wear tests under identical conditions (test conditions: load, 5 N; sliding velocity, 1 m/s; relative humidity, 35%; sliding distance, 2 km; temperature, 23°C; pin radius, 4.77 mm).

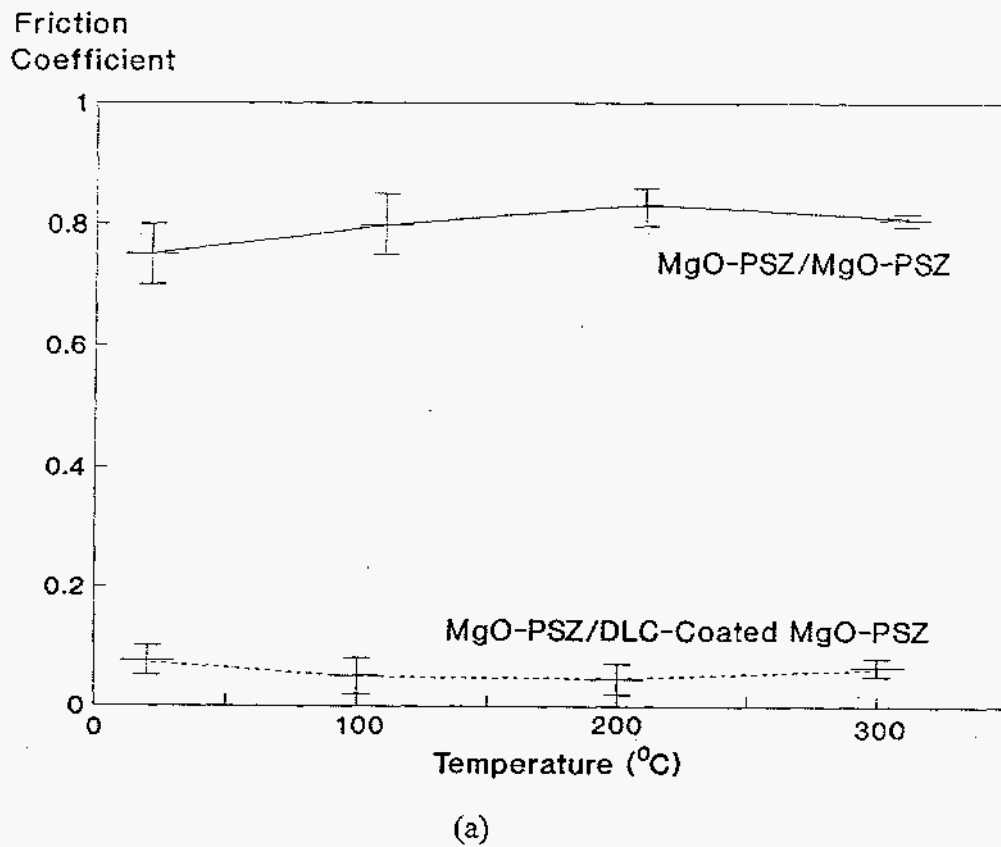


(a)

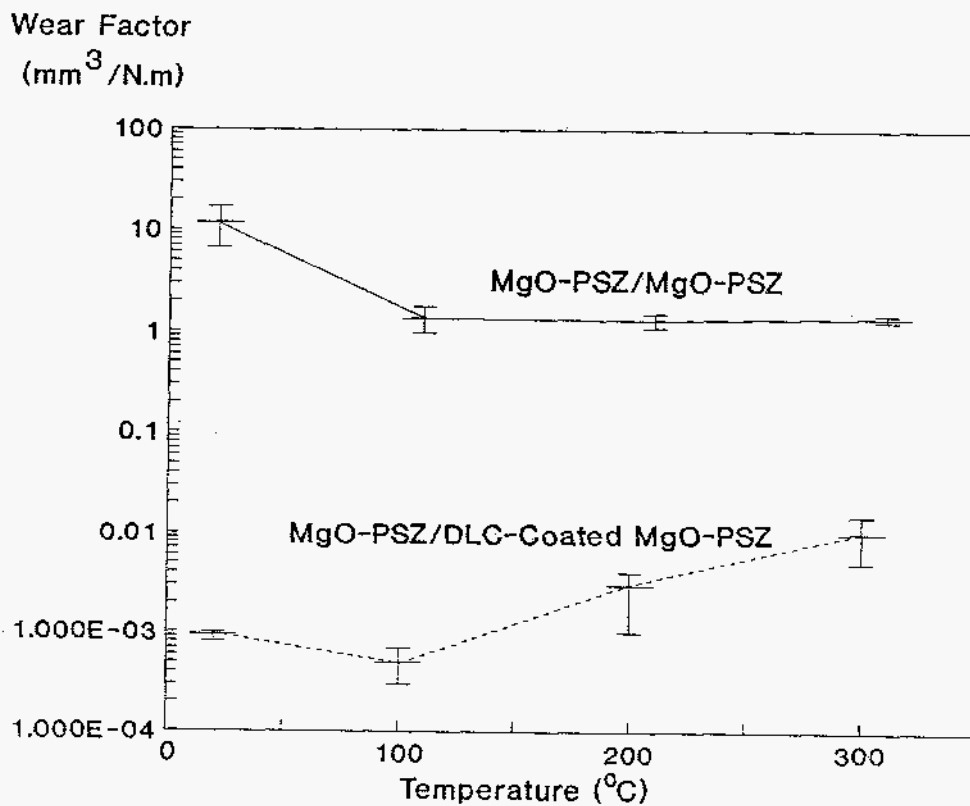


(b)

Figure 8. Effect of increasing load on (a) friction coefficients and (b) average specific wear rates of the MgO-PSZ balls during sliding against DLC-coated MgO-PSZ disks (test conditions: sliding velocity, 1 m/s; relative humidity, 35%; sliding distance, 2 km; temperature, 23°C; pin radius, 4.77 mm).

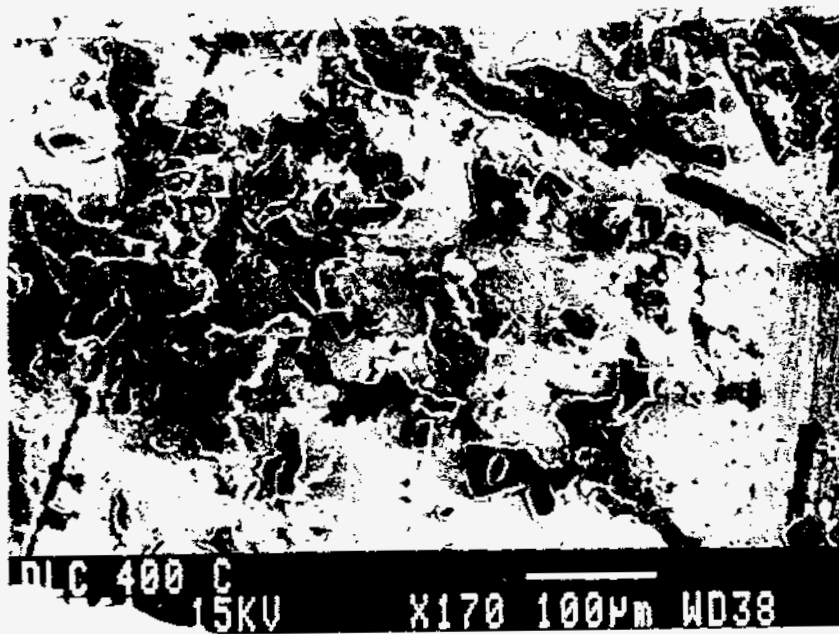


(a)

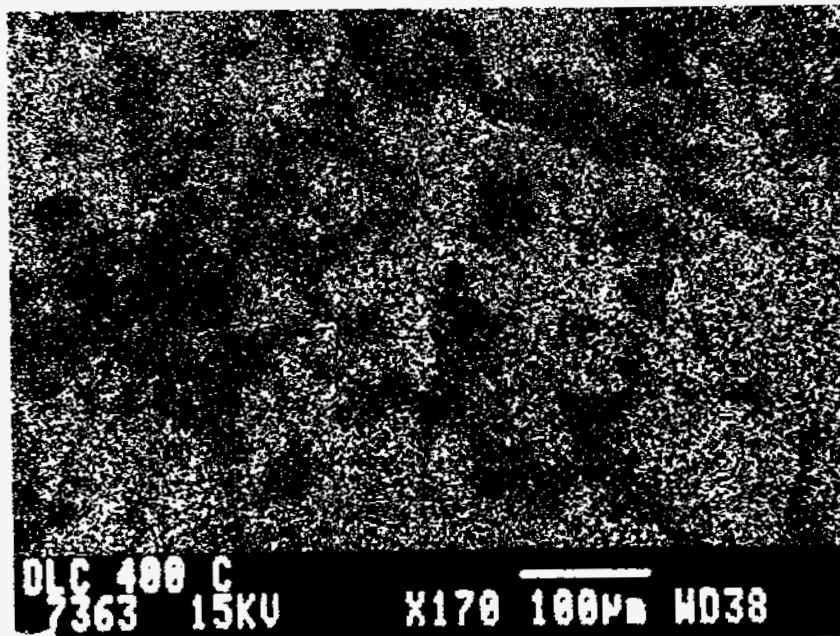


(b)

Figure 9. Effect of ambient temperature on (a) friction coefficients and (b) average specific wear rates of the MgO-PSZ balls during sliding against uncoated and DLC-coated MgO-PSZ disks (test conditions: load, 5 N; sliding velocity, 1 m/s; relative humidity, 35%; sliding distance, 2 km; pin radius, 4.77 mm).

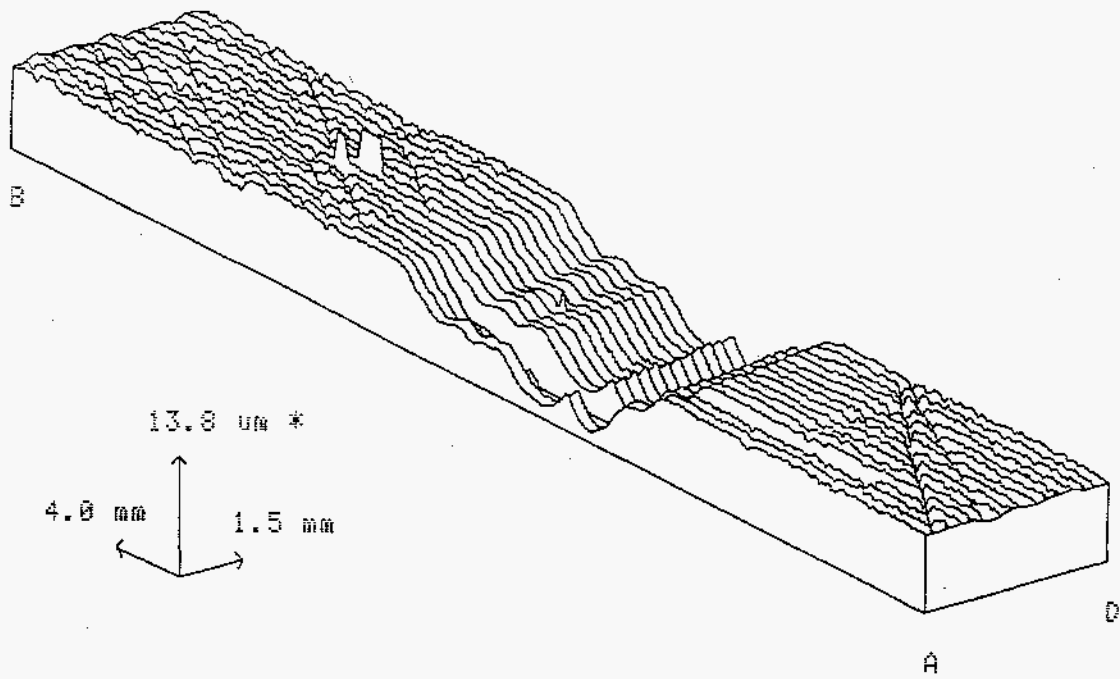


(a)

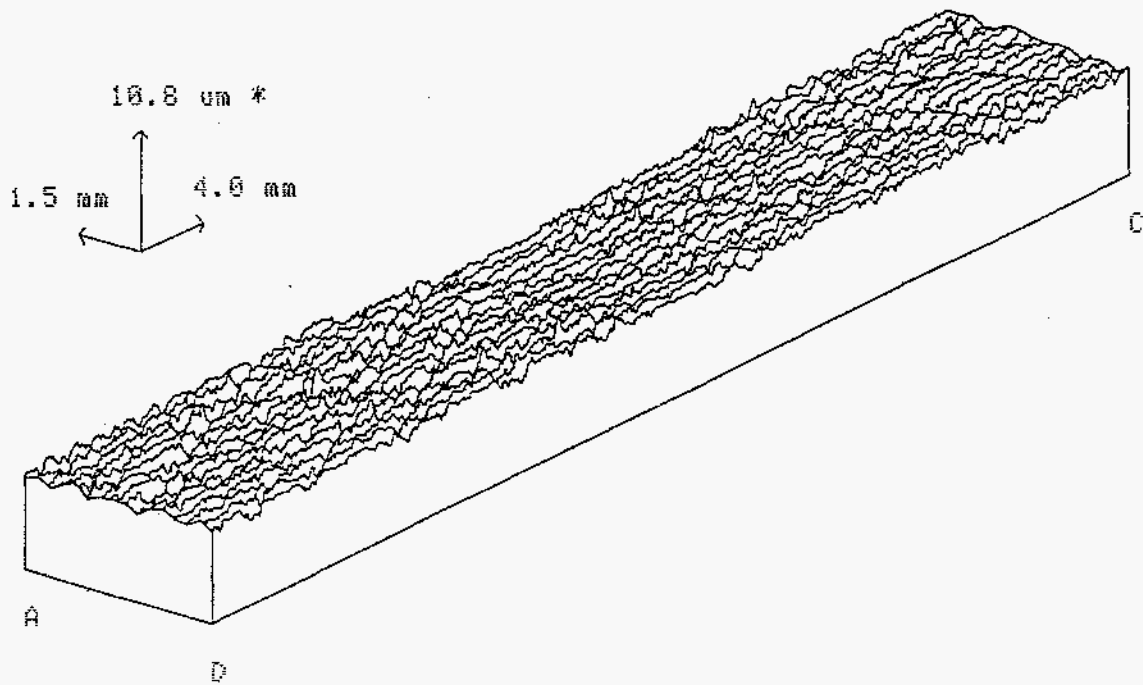


(b)

Figure 10. (a) SEM micrograph and (b) X-ray Zr map of a DLC-coated MgO-PSZ disk after exposure to 400°C test temperature.



(a)



(b)

Figure 11. 3-D surface maps of wear tracks formed on (a) uncoated and (b) DLC-coated MgO-PSZ disks during sliding against MgO-PSZ balls at 300°C (test conditions: load, 5 N; sliding velocity, 1 m/s; relative humidity, 35%; sliding distance, 2 km; pin radius, 4.77 mm).

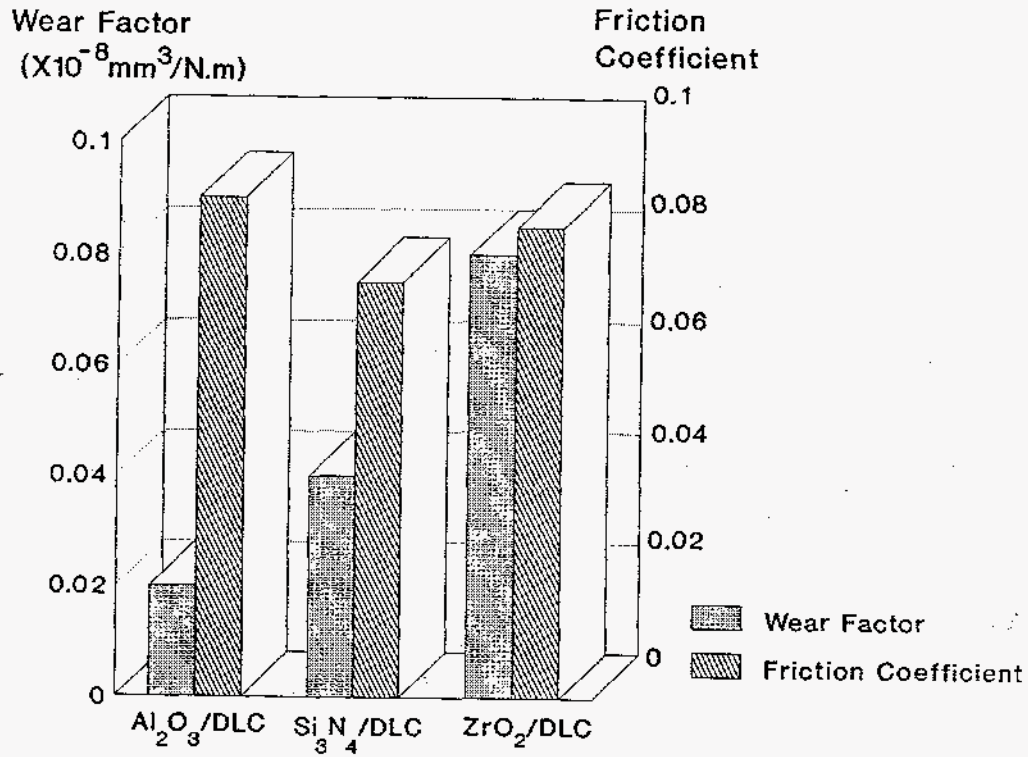
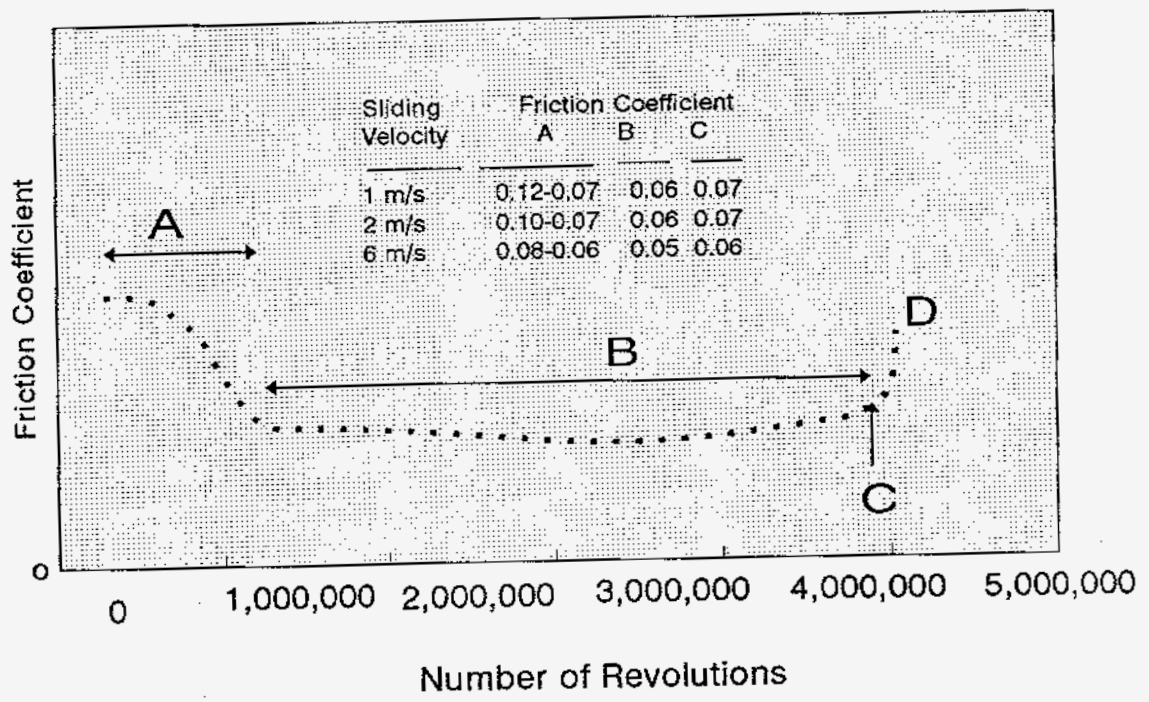
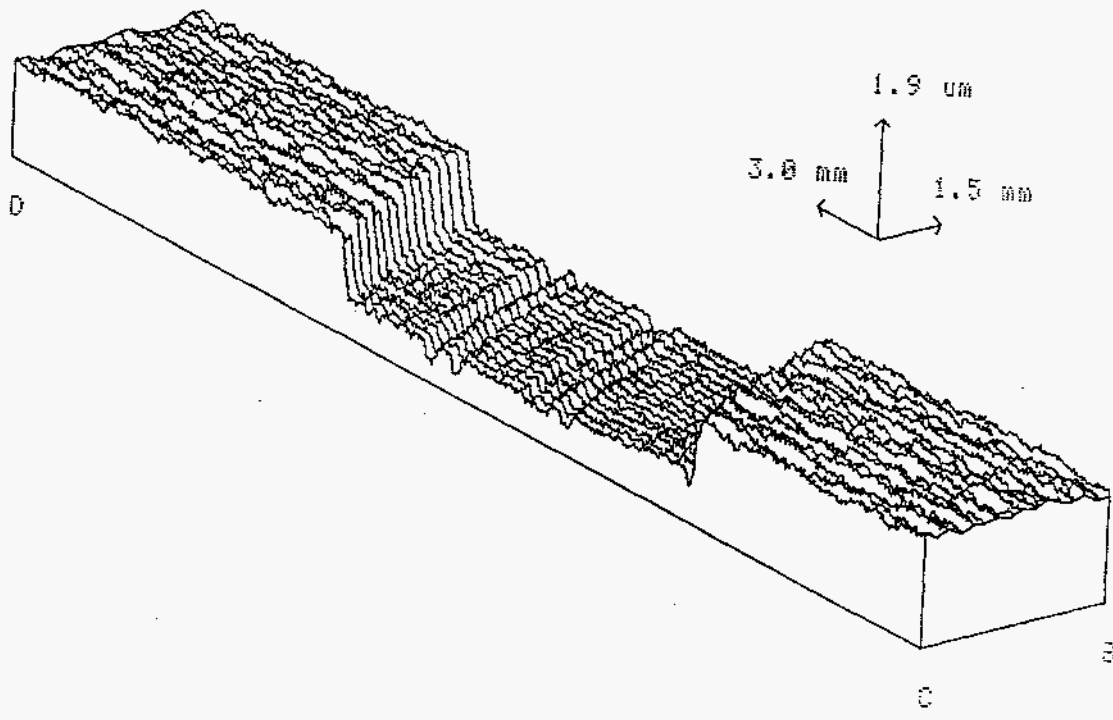


Figure 12. Friction coefficients and average specific wear rates of  $\text{Al}_2\text{O}_3$ ,  $\text{Si}_3\text{N}_4$ , and MgO-PSZ balls during sliding against DLC-coated MgO-PSZ disks (test conditions: load, 5 N; sliding velocity, 2 m/s; relative humidity, 35%; sliding distance, 2 km; pin radius, 4.77 mm).

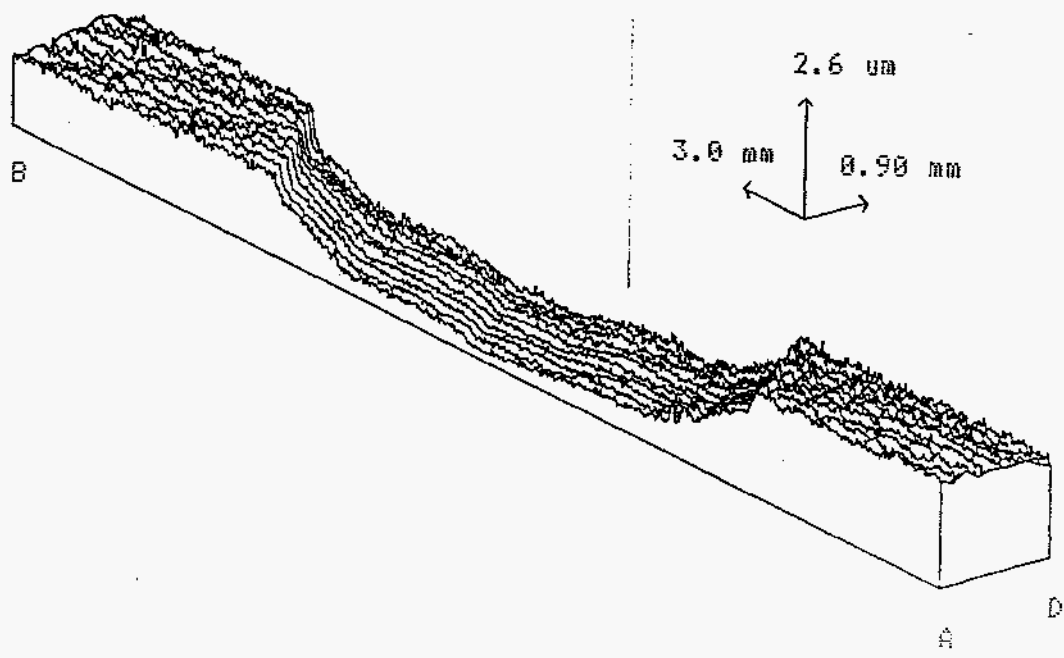


Sliding Velocity (m/s)	A	B	C	D	Ball Wear Rate (mm <sup>3</sup> /N.m)
1	520,000	3,430,000	3,950,000	4,100,000	7X10 <sup>-9</sup>
2	320,000	2,600,000	2,939,000	3,150,000	7X10 <sup>-9</sup>
6	200,000	1,100,000	1,370,000	1,420,000	3.3X10 <sup>-8</sup>

Figure 13. Friction and wear performance of DLC-coatings subjected to long-duration sliding tests at velocities of 1, 2, and 6 m/s (test conditions: load, 5 N; relative humidity, 35 to 50 %; pin radius, 4.77 mm; temperature, 23°C).



(a)



(b)

14. 3-D surface maps of wear tracks formed on DLC-coated MgO-PSZ disks during lifetime tests at (a) 1 m/s and (b) 6 m/s (test conditions: load, 5 N; relative humidity, 35-50%; pin radius, 4.77 mm).